



# **Transcript analysis reveals an extended regulon and the importance of protein-protein co-operativity for the *Escherichia coli* methionine repressor**

Ferenc Marincs, Iain W. Manfield, Jonathan A. Stead, Kenneth J. Mcdowall, Peter G. Stockley

## **► To cite this version:**

Ferenc Marincs, Iain W. Manfield, Jonathan A. Stead, Kenneth J. Mcdowall, Peter G. Stockley. Transcript analysis reveals an extended regulon and the importance of protein-protein co-operativity for the *Escherichia coli* methionine repressor. *Biochemical Journal*, 2006, 396 (2), pp.227-234. <10.1042/BJ20060021>. <hal-00478503>

**HAL Id: hal-00478503**

**<https://hal.science/hal-00478503v1>**

Submitted on 30 Apr 2010

**HAL** is a multi-disciplinary open access archive for the deposit and dissemination of scientific research documents, whether they are published or not. The documents may come from teaching and research institutions in France or abroad, or from public or private research centers.

L'archive ouverte pluridisciplinaire **HAL**, est destinée au dépôt et à la diffusion de documents scientifiques de niveau recherche, publiés ou non, émanant des établissements d'enseignement et de recherche français ou étrangers, des laboratoires publics ou privés.



HAL Authorization

**Transcript Analysis Reveals an Extended Regulon and the Importance of Protein-Protein Cooperativity for the *E. coli* methionine repressor**

Ferenc Marincs, Iain W. Manfield, Jonathan A. Stead,  
Kenneth J. McDowall and Peter G. Stockley\*.  
Astbury Centre for Structural Molecular Biology,  
University of Leeds, Leeds, LS2 9JT, U.K.

Running title: *E. coli* transcriptome analysis of a *metJ* knockout

Address correspondence to: Peter G. Stockley, Astbury Centre for Structural  
Molecular Biology, University of Leeds, Leeds, LS2 9JT, U.K.

Telephone: 0113-343-3092; Fax: 0113-343-7897; E-mail: [stockley@bmb.leeds.ac.uk](mailto:stockley@bmb.leeds.ac.uk)

Keywords: methionine biosynthesis; DNA-protein interactions; *in vivo* phenotype

Short title: Mutant *metJ* transcript analysis

-----

We have used DNA arrays to investigate the effects of knocking out the methionine repressor gene, *metJ*, on the *E. coli* transcriptome. We assayed the effects in the knockout strain of supplying wild-type or mutant MetJ repressors from an expression plasmid, thus establishing a rapid assay for *in vivo* effects of mutations characterised previously *in vitro*. Repression is largely restricted to known genes involved in the biosynthesis and uptake of methionine. However, we identified a number of additional genes that are significantly up-regulated in the absence of repressor. Sequence analysis of the 5' promoter regions of these genes identified plausible matches to met-box sequences for three of these, and subsequent EMSA analysis showed that for two such loci their repressor affinity is higher or comparable to the known *metB* operator, suggesting that they are directly regulated. This can be rationalised for one of the loci, *folE*, by the metabolic role of its encoded enzyme; however the links to the other regulated loci are unclear suggesting both an extension to the known *met* regulon and additional complexity to the role of the repressor. The plasmid gene replacement system has been used to examine the importance of protein-protein cooperativity in operator saturation using the structurally characterised mutant repressor, Q44K. *In vivo*, there are detectable reductions in the levels of regulation observed, demonstrating the importance of balancing protein-protein and protein-DNA affinity.

-----

## INTRODUCTION

The *E. coli* methionine repressor, MetJ, was the first structurally characterised member of the ribbon-helix-helix (RHH) class of DNA-binding proteins that interact with DNA bases via a pair of  $\beta$ -strands [1-9] (see Figure 1A). It was believed to bind at least seven operators [10] located in the 5' regions of genes involved in biosynthesis of methionine (Fig. 1B, C), most of which do not form operons and are dispersed in the genome [11], including the *metJ* gene [12]. Operators contain tandem repeats of an 8-bp sequence, the met-box, which varies around a consensus sequence of dAGACGTCT [13]. There are two to five such sequences tandemly repeated in natural operators [10]. The degree of identity with the perfect consensus is higher in the shorter operators and towards the centre of the longer operators [13, 14]. Interestingly, there are thought to be (see below) no perfect matches with even a single consensus met-box in *E. coli* operators, although *in vitro* affinity selection experiments [15] show that there is a clear preference for this sequence.

Crystallographic studies of various MetJ complexes have revealed the molecular basis for these observations. Each met-box is bound by a repressor dimer that also makes protein-protein contacts to neighbouring dimers leading to co-operative saturation of the operators [3, 13, 16]. Binding of two S-adenosylmethionine (AdoMet) co-repressor molecules to sites on the opposite side of the protein from the DNA-binding motif [2, 16] has been postulated to create an unusual long-range electrostatic interaction with the phosphodiester backbone of DNA, raising DNA affinity at least 100 fold [17] [18]. Sequence specificity arises via direct amino acid side chain hydrogen bonding to the bases at positions 2 and 3 in the met-box, and symmetry related positions in the larger operator, and via sequence dependent distortions of the operator duplex at the centre of met-boxes and at the junction between them [2, 3, 13]. Previously, we speculated that the natural operator sequence variation has arisen from the need to avoid cross-talk with the tryptophan repressor, TrpR, that has a consensus binding site with 50% identity to the sequence at the junction between met-boxes (-CTAG-) [13, 19, 20].

Very little is known about the mechanistic details of repression of the *met* genes *in vivo*. The large number of MetJ mutants studied to date *in vitro* potentially allow us to probe such details. For each mutant, however, there are possible effects on both repressor transcript and protein stability, as well as phenotypic effects on repression due to altered DNA affinity and discrimination, co-repressor binding and ability to form the higher order repression complexes. DNA microarrays offer an opportunity for screening all the effects of such mutations in the context of the genome. Previous reports have demonstrated that this technology is a powerful way to study gene expression in *E. coli* [21-29]. Here, we describe the effects of a *metJ* knockout on expression of the *met* regulon. Loci previously not known to be directly regulated are also detected and analysed *in vitro*. The regulation of some of these can be rationalised by the relationships of their encoded proteins to the *met* metabolome. The role(s) of protein-protein cooperativity in regulation was also investigated using a MetJ mutant (Q44K) characterised *in vitro* as having reduced cooperativity in operator saturation [30].

## MATERIALS AND METHODS

*Strains and plasmids.* Strains LU106 and LU118 containing chromosomal *metJ::Tn(kan)* and *trpR::Tn(kan)* knockouts, respectively, were generated by combining *in vitro* transposon mutagenesis ([http://www.epicentre.com/guide\\_to\\_transposomics.asp](http://www.epicentre.com/guide_to_transposomics.asp)) with lambda (red)-mediated *in vivo* recombination [31] in DY378 cells [32].

Plasmids were constructed by PCR amplification of appropriate chromosomal segments of DNA, encoding either the entire *metJ* gene and *metB* promoter region (pFM20) or just the *metB* promoter (pFM26), followed by insertion into plasmid pGFP (Clontech), so that the *metB* promoter in each case was driving transcription of the gene for green fluorescent protein. pFM20 encoded *metJ* was then mutated using the QuikChange Site-Directed Mutagenesis Kit (Stratagene). The presence of the desired mutation was confirmed by sequencing the resulting plasmid designated pFM45 (*metJ*Q44K). The details of the primers used for these and other constructions described here are given in Table 4 of the Supplementary Material.

*Microarrays.* A multipurpose PCR-based microarray of 73 *E. coli* genes (Supplementary Material, Table 5) encompassing known structural and regulatory genes of the *met*, *trp*, *arg* regulons,  $\sigma^{54}$ -regulated genes and a number of ribonucleases and their target genes was designed and constructed. Manufacturing of the microarray is described in detail in the Supplementary Material. We also used an oligonucleotide-based array from MWG that contains 50-mer oligonucleotides representing 4,288 *E. coli* genes. The layout of this array can be downloaded from [http://ecom2.mwgdna.com/download/arrays/arrays/gene\\_id/html/gene\\_id\\_ecoli\\_v2.html](http://ecom2.mwgdna.com/download/arrays/arrays/gene_id/html/gene_id_ecoli_v2.html).

*RNA isolation and cDNA synthesis.* For each experiment described here, three cultures of each strain were grown in parallel. RNA was isolated from each culture and fluorescently-labelled cDNA synthesised. Each strain was grown at 37°C with shaking (200 rpm) in 50 ml of LB supplemented with methionine or tryptophan or both (100  $\mu\text{g ml}^{-1}$ ) as appropriate, and ampicillin (100  $\mu\text{g ml}^{-1}$ ) when it contained a pFM plasmid. When the  $A_{660\text{ nm}}$  was 0.5-0.6, a 30-ml aliquot was added to 4 ml of stop solution (5 % v/v phenol in ethanol), the mixture split into 2 ml aliquots and the cells harvested by centrifugation at 4°C and 13,000 rpm for 2 min. The supernatant was removed and the pellets stored at -80°C, if not used immediately.

Total RNA was isolated from single frozen pellets using the NucleoSpin RNA II Kit (Macherey-Nagel) and then cDNA synthesised and labelled using Cy3 or Cy5 dCTP (Cy-dCTP) in the presence of random hexamers (10  $\mu\text{g}$ ) and total RNA (2.5-5  $\mu\text{g}$ ) in a total volume of 25  $\mu\text{l}$ . The mixture was incubated at 65°C for 10 min followed by 10 min at room temperature. Reverse transcription was performed at 42°C for 2 hours in 40  $\mu\text{l}$  reaction volumes containing 1x Superscript II buffer, 10  $\mu\text{M}$  DTT, 62.5  $\mu\text{M}$  dATP, dGTP and dTTP, 25  $\mu\text{M}$  dCTP and 50  $\mu\text{M}$  Cy-dCTP (Amersham, UK), and 400 U Superscript II (Invitrogen). The labelled cDNA was then purified using a MiniElute PCR purification kit (Qiagen).

*Microarray hybridisation and data analysis.* Labelled cDNA was dried, dissolved in 40  $\mu\text{l}$  of microarray hybridisation buffer (MWG); 50% (v/v) formamide, 6 x SSC,

0.5% (w/v) SDS, 50 mM sodium-phosphate and 5x Denhardt's reagent, and denatured at 95°C for 3-5 min. The denatured sample was applied to the microarray, covered with a plastic slip (Hybri-Slips, Sigma) and hybridisation performed in a sealed chamber (MWG) submerged in a 42 °C water bath for 18 hours. Slides were then washed for 5 min at RT in 2 x SSC, 0.1% (w/v) SDS; 1 x SSC 0.1% (w/v) SDS and 0.5 x SSC, dried under compressed air and scanned using an Affymetrix 418 scanner at 100% laser power and 20-50% gain settings.

The raw images were analysed using ArrayPro software (Media Cybernetics, USA). Signals from the miniarray were normalised to a set of genes involved in the biosynthesis of arginine, the decay of mRNA and the processing of ribosomal RNA, or known to be regulated post-transcriptionally, using the bicubic polynomial normalisation function of the software. The average ratio and standard deviation (SD) values from three parallel slides were calculated in Excel (Table 6 in Supplementary Materials).

The same RNA samples that were analysed using the mini-array were labelled as described above, mixed together, and hybridised to the whole genome array. Following the method of Dudoit *et al.* [33], we plotted the log ratio of each gene ( $\log_2(\text{Cy3}/\text{Cy5})$ , the M value, against the average of the log signal ( $0.5 \times (\log_2 \text{Cy3} + \log_2 \text{Cy5})$ , the A value. The M values were then normalised using LOWESS, which uses locally weighted regression to smooth scatter plots [34]. To identify ratio values that were outside the 'noise' of the oligonucleotide array system and therefore more likely to be of biological significance, the data were sorted from the lowest to the highest A value, and the standard deviations of the normalised M values in a sliding window of 50 genes were used to define the boundaries of the noise envelope of the scatter plot [35]. Normalised values of M that were outside this noise envelope were considered to be more likely of biological significance. The normalised ratio values (i.e. the non-log data) for genes found to be repressed and outside the noise envelope in three out of three experiments are provided in Table 2 and in Supplementary Materials, Table 7.

*Two-step reverse-transcription PCR.* Unlabelled cDNA was synthesised in a similar way as described above for fluorescently-labelled cDNA, with the following

modifications; only 50 ng RNA was used per reaction, no Cy-labelled nucleotide was present, and all four nucleotides were at 62.5  $\mu$ M in the reaction. The reactions were primed by adding either random hexamers (10  $\mu$ g) or gene-specific primers to 50 nM. 1  $\mu$ l aliquots of the reverse transcription reaction were used in the PCR step. To control for DNA contamination in the RNA samples, Superscript II reverse transcriptase was omitted from the RT step. For PCR in this particular experiment, and throughout the entire work, we used the REDTaq Ready Mix PCR reaction mix (Sigma), and 0.2  $\mu$ M of primers. Conditions for PCR were: 30 cycles of 30 sec at 92°C, 30 sec at 55°C and 1 min 40 sec at 72°C, followed by an extension step of 10 min at 72°C.

*SPR assays.* DNA fragments for SPR analysis were amplified by PCR and immobilised on BIAcore SA chips using standard procedures. For the *metE* promoter-operator (Figure 1B) care was taken to construct fragments encompassing only the full *metR* or *metE* promoters in each case, thus avoiding complications from having two RNAP binding sites on each fragment. A separate fragment, lacking a promoter, but encompassing the downstream operator, *metE<sub>down</sub>*, was also produced. More details about these constructs are given in Table 8 of Supplementary Materials, RNAP holoenzyme was purchased from Epicentre Technologies and used as supplied. MetJ was purified following standard procedures and dialysed against analysis buffer (AB; 20 mM Tris-HCl, pH8.0, 150 mM NaCl, 10 mM MgCl<sub>2</sub>, 1 mM DTT) before use. Interactions of RNAP and MetJ with DNA were analysed in AB + 0.005%(v/v) surfactant P20 with saturating AdoMet (1 mM) added to MetJ binding reactions. Titrations were performed at least twice over a range of protein concentrations. Data from sensorgrams were corrected by subtraction of data from an underivatized flow cell and then fitted to a 1:1 Langmuir binding model to provide apparent association and dissociation rate constants ( $k_a$  and  $k_d$ ) and the equilibrium binding constant ( $K_D$ ).

*Electrophoretic Mobility Shift Assays (EMSA).* *In vitro* MetJ binding to putative operators was analysed by EMSA following procedures described previously [13].

## RESULTS

*Effects of the metJ knockout on the E. coli transcriptome.* In order to probe the extent of the *met* transcriptome and levels of regulation due to MetJ, we prepared total RNA from LU106, a *metJ* knockout strain, carrying either pFM20, a medium-copy-number plasmid that encodes wild-type *metJ*, or pFM26, a related control plasmid (see Materials & Methods). Cells were grown in Luria Broth to which methionine had been added to ensure that repression was effective. RNA samples were isolated during the middle of exponential growth and used as templates for the synthesis of cDNA. The cDNA samples, labelled with the fluorescent dyes Cy3 and Cy5 respectively, were mixed together and hybridised to an oligonucleotide-based array corresponding to all the 4,288 known genes and putative protein-coding regions of *E. coli* (MWG, Supplementary Material).

Since the slides used in these assays have only single spots for each gene, we used a robust statistical method to define a noise envelope for the data from each slide after normalisation (see Materials and Methods), and selected only those ratios that were outside the noise in three of three experiments and thus most likely to be biologically significant. 20 genes with average expression ratios >1.7-fold are listed in Table 1. As expected this list contains several known *met* genes; *metE*, *B*, *F*, *K*, *A* and *R*. We did not detect significant changes in the mRNA levels of *metC* and *metL* using this array (see below).

Among the other genes up-regulated in the absence of *metJ* was *folE* (~4x), which was also found to up-regulated (~4.5x) using a PCR-based array (see below and Table 6 in Supplementary Material). The product of this gene is involved in providing the co-factor for the final step of methionine biosynthesis (Figure 1C). Up-regulation of two other genes, *abc* (~2.5x) and *yaeE* (~5x) (recently re-named *metN* and *metI*, respectively), was also observed. These form an operon at the *metD* locus, encoding genes involved in methionine transport [36]. Our finding is consistent with those by others that the promoter upstream of *metN* is more effective at directing transcription of a *lacZ* reporter construct (2-12 fold) in the absence of either methionine in the growth medium or a functional *metJ* gene, and was reported to have at least two adjacent 8-bp sequences that share 100 and 62.5% identity with the met-box



consensus [37]. MetJ is clearly involved in the regulation of methionine uptake as well as biosynthesis. The third gene, *yaeC* (*metQ*) of the *metD* locus was found to be only slightly up-regulated (~1.5x) consistent with results obtained using a *lacZ* reporter fusion [36]. The *yaeC* gene is transcribed by its own promoter, which appears to lack met-box sequences. The modest up-regulation of this gene that we and others have found suggests that MetJ may influence transcription of a promoter that is downstream from (in the direction of transcription), but not in the close vicinity of its binding site.

The significance of the up-regulation of the other genes in Table 1 is not known. In order to determine whether the observed effects were due to direct regulation by the repressor or resulted from indirect effects, we searched for sequences similar to met-boxes in regions most likely to control the transcription of the non-*met* genes that were derepressed (Table 1). Using RegulonDB [38], we identified for each of these genes the position of either known or predicted promoters. Along with 200 bp of flanking DNA on either side, these promoter regions were screened individually using a sequence profile representing a tandem repeat of all known met-boxes to identify sequences with the most similarity. This was done using PROFILE and associated programs within the GCG Wisconsin Package (Accelrys Inc., San Diego).

Matches that appeared as similar to the profile as known *met* operators were obtained within regions upstream of *metN*, *folE*, *cspA* and *yaeS* (Fig. 2 legend) but not the other non-*met* up-regulated genes in Table 1. Met-box-like sequences overlapped the -35 box of the predicted  $\sigma^{70}$  promoter of *folE*. A pair of met-box-like sequences was centred 14 bp downstream of the known  $\sigma^{70}$  promoter of *cspA* [39] and the met-box-like sequences associated with *yaeS* were centred 206 bp upstream of a predicted  $\sigma^{70}$  promoter. Double-stranded oligonucleotide fragments encompassing these putative met-boxes for the *folE*, *cspA* and *yaeS* promoters were then synthesised and *in vitro* binding to MetJ analysed using electrophoretic mobility shift assays [13]. We were able to detect binding to all these fragments under conditions in which a *metC* oligonucleotide, with two met-boxes, shifted as expected for a fragment with an apparent  $K_D$  of ~4 nM dimer [13]. The affinities of these loci were *folE* – 30-40 nM, *cspA* – 30 nM and *yaeS* - >200 nM, MetJ dimer respectively. These are lower than

most of the known regulon, with the exception of *metB* (Table 8 in Supplementary Material) that has a  $K_D$  of ~40 nM dimer, suggesting that at least two of the additional loci are directly regulated by MetJ.

*Effects of the wild-type metJ gene within the known met regulon.* The effects of *metJ* on transcription within the *met* regulon were also investigated by comparing LU106 with DY378, its congenic wild-type partner, using a PCR-based array (Supplementary Material) consisting of multiple spots of 73 amplified ORF fragments corresponding to all of the known regulatory and structural genes of the *met* regulon, and a selection of other *E. coli* genes including several tryptophan biosynthetic (*trp*) genes (see below). Genes involved in the biosynthesis of arginine, the decay of mRNA and the processing of ribosomal RNA, or known to be regulated post-transcriptionally, were used for normalisation as they had no known links to the *met* regulon. As a control, we also reanalysed RNA from LU106 containing pFM20 or pFM26.

The expression ratios for the known *met* regulon derived from three independent comparisons of the strains are shown in Table 2. Note, these assays only identify relative changes in gene expression at each locus sampled; they do not record absolute levels of transcript produced, but this is not necessary for probing repressor function. The level of the mutated *metJ* transcript was found to increase 2.6 fold in LU106 compared to DY378, consistent with disruption of the known auto-regulation of this gene [12]. Five of the *met* biosynthetic genes (*metA*, *metB*, *metC*, *metF*, and *metK*) were derepressed more than 2 fold in the knockout strain. Other *met* genes displayed only moderate changes and these may well be within the experimental error of these assays. The *metR* gene, which activates *metE* and *metH*, was only slightly derepressed. The *metH* gene lacks a met-box in its promoter region and this is consistent with its expression ratio of ~1.0. The ratio for *metG* was also very close to 1. The most strongly regulated loci were *metA*, *metF* and *metK*.

The *metA* gene encodes a homoserine transsuccinylase, which converts L-homoserine into O-succinyl homoserine in the fourth step of the pathway. The *metF* gene encodes a methylene tetrahydrofolate reductase that catalyses reduction of  $N^5,N^{10}$ -methylenetetrahydrofolate to  $N^5$ -methyltetrahydrofolate, a cofactor in the

homocysteine to methionine conversion step. The *metK* gene encodes methionine adenosyl transferase, the enzyme that synthesises the co-repressor, AdoMet, and was previously identified as a likely regulation target on the basis of bioinformatic analysis [40]. Therefore, two steps involved in the production of the end-products of the biosynthetic pathway (Figure 1C) appear to be repressed the most by MetJ.

The other two genes derepressed more than 2-fold were *metB* and *metC*. The *metB* gene forms, with *metL*, the only known operon of the *E. coli* *met* regulon. The *metB* and *metC* gene products are involved in intermediate steps of methionine biosynthesis, while *metL* encodes a homoserine dehydrogenase, which is the first enzyme in the pathway. The expression ratio for *metL* is ~2-fold lower than that of *metB* even though the two genes are co-transcribed. Differences in ratios for genes within an operon have been observed previously, e.g. *lacZYA* [41], and may reflect either biological differences in the decay of segments of polycistronic mRNA under different conditions or technical differences such as the stringency of hybridisation to immobilised probes. Assuming the latter is not a problem here, these results suggest that MetJ acts to lower rather than block the flux through the methionine biosynthetic pathway, since if no transcripts were produced when repression was effective the expression ratios would be expected to be much higher. Other unrelated genes on the array showed no significant changes in gene expression (Table 6 in Supplemental Material).

The number of RNA polymerase molecules in an *E. coli* cell is estimated to be ~2000. These are in competition with the estimated ~600 molecules of MetJ for access to the regulated promoters. The intrinsic affinity of each of these species for their binding sites at each locus could, in principle, be the basis of the differential expression ratios observed. We therefore measured apparent association and dissociation rate constants for operator binding, and thus the apparent equilibrium constants, for both repressor and holo-RNA polymerase binding to immobilised DNA fragments encompassing the promoter regions of the various *met* loci *in vitro* using SPR [18, 42-44]. The results (Table 8 in Supplementary Material) show no clear correlation between the apparent affinities, on- or off-rate constants and expression ratios. These results imply that the primary transcript levels are determined by the rate of isomerisation of the bound RNAP molecules at the different promoters.

*metE* is uniquely sensitive to the dosage of *metJ*. The *met* expression ratios for LU106 (pFM20) vs. LU106 (pFM26) on the PCR-based array were similar to the results obtained using the full array, although their rank order was slightly different and we did not detect significant changes in the mRNA levels of *metC* and *metL* using the latter (Table 1). Such non-correlations between different types of arrays have been reported previously [45] and in our case likely reflect differences in the efficiency and/or specificity of hybridisation of cDNA to oligonucleotide and PCR-generated probes. Surprisingly, increased gene dosage had a dramatic effect on the expression ratio of just one *met* gene. In the knockout strain *metE* was only derepressed 1.3 fold compared to the wild-type but this value was ~38 fold when LU106 (pFM26) and LU106 (pFM20) were compared. *metE* is unique amongst the known *met* genes in having two operator sites (Fig. 1B); one encompassing a set of three met-boxes and a second with a set of four, centred 15 bp and 113 bp, respectively, upstream of the *metE* transcriptional start site (Figure 1). The results suggest that increasing the concentration of MetJ in LU106 (pFM20) leads to saturation of both these operators, implying that under more physiological concentrations of repressor they are not saturated. This unexpected result has the benefit that the depression ratio of *metE* becomes very sensitive to the functions of the *metJ* mutants to be tested.

More modest differences (<2-fold) were also observed in the depression ratios of other *met* genes. While the explanation for the increase in the expression ratio for *metE* can be explained by increased occupancy of operators, it is unlikely to be the explanation for the decrease in the ratios observed for *metA* and *metK*. It is not possible given the complexity of living cells and the interconnection of physiology and gene regulation to ascribe a particular molecular explanation to these relatively small effects. Despite the increased MetJ levels no other loci appeared to be affected apart from *folE* (see above)(Supplemental Material, Table 6) confirming the sequence discrimination of the protein.

To verify the apparent changes in gene expression described above in the plasmid based system, we compared the relative mRNA levels of the *met* genes in LU106 (pFM26) and LU106 (pFM20) using end-point RT-PCR. The results, although only qualitative (Figure 3), confirmed the overall pattern, *i.e.* with the exception of *metG*

mRNA, the transcript levels of all of the *met* genes were lower in the presence of plasmid-encoded MetJ. Moreover, *metE* and *metF* were the only genes for which we were unable to detect transcripts in cells containing pFM20 (Table 2, Fig. 3), consistent with their higher expression ratios. Under the conditions used RT-PCR was able to detect mRNA corresponding to wild-type *metJ* in LU106 (pFM20) but not transcripts corresponding to mutated *metJ* in LU106 (pFM26).

*Probing met and trp cross-talk.* Tandem consensus met-boxes share sequence identity with operator sites recognised by the helix-turn-helix motif of the TrpR repressor [13, 14, 19], and both operators have 8-bp repeats of these recognition sites. This led us previously to suggest that TrpR might bind to its operators in the same tandem fashion as MetJ, and that the two regulatory proteins might cross-talk between regulons [14, 19]. The first of these suggestions was spectacularly borne out by the determination of the crystal structure of a tandemly bound TrpR complex in which the N-terminal arms of the protein were visible in the electron density maps [19] [46], having been disordered in previous structures containing only a single dimer bound to DNA. We therefore used the PCR gene array to examine the separate effects of *trpR* and *metJ* knockouts on the expression of the *met* and *trp* genes.

We generated a *trpR* knockout strain (LU118) by the same *in vitro* transposon mutagenesis procedure [31] and investigated the expression ratios of the genes on the array compared to the wild-type strain (DY378). The ratios were 3.3 (3.8), 2.4 (4.1), 2.9 (4.4), 2.0 (3.7), 2.7 (6.3), 1.0 and 0.8 for *trpA*, *trpB*, *trpC*, *trpD*, *trpE*, *trpR* and *trpS*, respectively. The figures in brackets are the reported values, where available, from Yanofsky and co-workers obtained using a *trpR* frame-shift mutant in strain CY15682 [28]. Expression of the *trpR* and *trpS* genes was not affected, nor were any of the *met* genes affected (expression ratios 0.8-1.0). In the equivalent *metJ* knockout experiment, i.e. LU106 versus DY378, none of the *trp* genes were affected (ratios 0.9-1.0), while the overall pattern of the expression ratios of the *met* genes were as described above (Table 2). These results suggest that wild-type *met* and *trp* repressors do not cross-talk to each other's regulons.

*Probing the roles of protein-protein cooperativity in operator saturation in vivo.*

Having established the effect of expressing wild-type *metJ* from a plasmid, we used the same approach to probe the effect(s) of introducing the MetJ Q44K mutant, which has altered protein-protein cooperativity [30]. The plasmid pFM45, encoding the Q44K mutant, was created by site-directed mutagenesis of pFM20 and then introduced into LU106, and the transcript levels in these cells compared with LU106 (pFM20). In the Q44K mutant the level of the *metJ* transcript was ~7x higher (Table 3) consistent with the cooperativity of binding of MetJ dimers having a significant role in autoregulation [30]. This result also suggests that the cellular concentration of Q44K is likely to be substantially higher than that of wild-type MetJ. However, despite this all of the *metJ*-regulated genes are repressed less well in cells expressing Q44K, whilst no other genes in the array showed significant changes (Supplemental Material, Table 6). The largest change in expression ratio is for *metE* (~6 fold). This value should be compared to the ~38 fold ratio for the plasmid-containing strains. We would expect the two *metE* operator sites (Fig. 1B) to be particularly sensitive to altered protein-protein cooperativity because of their poor identity to the consensus met-box sequence that is presumably compensated by the protein-protein interactions possible in an extended operator. These data confirm for the first time that the co-cooperativity of binding of MetJ dimers has a significant role in the regulation of all the known MetJ-regulated genes *in vivo*.

## DISCUSSION

The results described above illustrate how *in vivo* transcript analysis can be used to extend *in vitro* structure-function studies of DNA regulatory proteins. The first detailed analysis of changes in gene expression levels when *metJ* is deleted, together with the SPR determination of affinities for holo-RNAP and MetJ binding at the various promoter-operator sites, suggests that only modest repression normally occurs at regulated promoters and that this can not simply be inferred from *in vitro* binding assays. Two aspects of the results were unexpected. Firstly, when we replaced the knockout with a wild-type *metJ* gene expressed from a plasmid, thus increasing gene copy number, transcript and presumably repressor protein concentrations, there was a remarkable increase in the ability of MetJ to repress the *metE* locus. This can be rationalised by assuming that the unique double operator structure at this locus is not normally saturated by repressor, presumably because of their low identity to consensus met-boxes. In principle therefore, *metE* transcripts alone could be used to

look at the effectiveness of mutant repressors. However, the transcript assays are more powerful because they allow simultaneous assessment of loss of sequence discrimination, *e.g.* by examining the idea that MetJ and TrpR might cross-talk between their regulons.

A second interesting observation came from examining the effects of *metJ* knockout on the entire transcriptome. This identified several genes within the methionine regulon that have only recently been characterised, as expected, but it also highlighted previously unknown, potentially regulated loci. Bioinformatic analysis of the promoter regions of these genes suggested that three of them could contain met-box sites and this has been confirmed by EMSA assays. The retarded species for *folE*, *cspA*, and *yaeS* at high concentrations of repressor, had lower mobility than the *metC* complex being formed, consistent with the presence of more than two met-boxes at these sites (Fig. 2). Binding into adjacent 8 bp sites that have partial matches to the met-box consensus is a well-known property of the repressor and is consistent with the sequences concerned. This is not seen with *metC* due to its high identity with the consensus allowing it to become fully shifted at lower protein concentrations.

For *folE*, there is a clear explanation of the newly discovered regulation in terms of the methionine biosynthesis pathway (Fig. 1C), the encoded enzyme providing a vital co-factor for the final step of AdoMet biosynthesis. For the other genes that bind MetJ, *yaeS*, also known as *uppS*, encodes undecaprenyl pyrophosphate synthetase (EC 2.5.1.31) (UPP synthetase) that generates UPP, a precursor in the biosynthesis of bacterial cell wall polysaccharide components, from isopentenyl pyrophosphate. *cspA* is known to encode a cold shock protein that can act as a chaperone. The relationship of either of these genes to the *met* metabolome is unclear, hinting at a previously unrecognised complexity. The coupling of the *metJ* knockout on the expression of other genes lacking obvious met-box sites we assume is a result of indirect effects (Table 1).

Previously, the *E. coli* genome has been analysed for putative MetJ binding sites. Two approaches have been adopted. The first used genomic SELEX to isolate DNA fragments with high affinity for the repressor *in vitro* [47], whilst the second used a bioinformatics approach that takes into account similarity in the predicted

conformation of DNA as well as its primary sequence [40]. Outside of the previously known *met* regulon, the majority of the putative interactions identified by these approaches were not confirmed by our data. However, the array empirically identified all known MetJ-regulated loci and three additional sites not highlighted by these previous studies. Genomic SELEX assays could have failed to detect the new sites due to their relatively low repressor affinity or because *in vivo* DNA affinities are modulated by other factors than in an *in vitro* EMSA. The failure of the bioinformatic approach suggests that even in a very well characterised system it is very difficult to define the conformational requirements for protein-DNA binding *in silico*. We cannot exclude the possibility, however, that genes other than the ones identified here are regulated by MetJ under different growth conditions.

The plasmid based transcript system was then used to probe the effects of a mutation within MetJ, Q44K, that leads to an altered pattern of met-box binding *in vitro*. The Q44K protein forms stable complexes with single met-box sites but will also form the higher order species on longer operator sites [30, 48], i.e. *in vitro* it can make a DNA complex without the protein-protein interaction normally seen in the minimal two met-box operators. Crystal structures of the singly bound dimer show that the introduced K44 side chain makes an additional intermolecular contact to the DNA backbone and that the orientation of the protein dimer along the DNA is such that it would have to undergo a rearrangement before it could participate in the higher order complex. We have suggested that this complex may represent an intermediate on the pathway to operator saturation [30]. Affinity measurements show that it binds the longer sites 75-95% as well as the wild-type repressor, the reduced binding apparently being due to the energetic cost of the conformational rearrangement that is required to convert the singly bound species to the higher order one. We anticipated therefore that these properties of the Q44K mutant might alter both *in vivo* affinity and DNA specificity. However, although the *met* genes are regulated less well by Q44K compared to the WT (reflecting reduced affinity and the importance of the protein-protein co-cooperativity), there is no effect on genes outside the *met* regulon suggesting no loss of sequence discrimination during binding.



The results described here suggest that relatively subtle functional effects are easily detectable *in vivo*, allowing us to probe the physiological requirements of balancing DNA affinity and protein-protein co-cooperativity in this system.

## ACKNOWLEDGEMENTS

We thank Prof. Donald Court for the gift of strain DY378, Drs. Chi Trinh and Tamara Belyaeva for preparing Figures 1A and 2, respectively, and Mrs Jenny Baker for expert technical assistance. We acknowledge the UK BBSRC and The University of Leeds for support of this work. KMD was the recipient of a Royal Society University Research Fellowship; JAS was supported by a BBSRC studentship.

## REFERENCES:

1. Phillips, S.E.V. (1991). Specific b-sheet interactions. *Curr Opin Struct Biol* 1, 89-98.
2. Somers, W.S., and Phillips, S.E.V. (1992). Crystal structure of the met repressor operator complex at 2.8Å resolution: DNA recognition by b-strands. *Nature* 359, 387-393.
3. He, Y.Y., McNally, T., Manfield, I., Navratil, O., Old, I.G., Phillips, S.E.V., Saint Girons, I. and Stockley, P.G. (1992). Probing met repressor operator recognition in solution. *Nature* 359, 431-433.
4. Bowie, J.U., and Sauer, R.T. (1990). TraY proteins of F and related episomes are members of the Arc and Mnt repressor family. *J Mol Biol* 211, 5-6.
5. Brown, B.M., Bowie, J.U. and Sauer, R.T. (1990). Arc repressor is tetrameric when bound to operator DNA. *Biochemistry* 29, 11189-11195.
6. Breg, J.N., van Ophersden, H.J., Burgering, M.J.M., Boelens, R., and Kaptein, R. (1990). Structure of Arc repressor in solution: evidence for a family of b-sheet DNA binding proteins. *Nature* 346, 586-590.
7. Raumann, B.E., Brown, B.M., and Sauer, R.T. (1994). Major groove DNA recognition by b-sheets: the ribbon helix helix family of gene regulatory proteins. *Curr Opin Struct Biol* 4, 36-43.
8. Gomis Rüth, F.X., Sola, M., Acebo, P., Parraga, A., Guasch, A., Eritja, R., Gonzalez, A., Espinosa, M., del Solar, G. and Coll, M. (1998). The structure

- p of plasmid encoded transcriptional repressor CopG unliganded and bound to its operator.
- EMBO J*
- 17, 7404-7415.
9. Chivers, P.T., and Sauer, R.T. (1999). NikR is a ribbon-helix-helix DNA-binding protein. *Protein Sci* 8, 2494-2500.
  10. Old, I.G., Phillips, S.E.V., Stockley, P.G. and Saint Girons, I. (1991). Regulation of methionine biosynthesis in the Enterobacteriaceae. *Prog Biophys Molec Biol* 56, 145-185.
  11. Old, I.G., Saint Girons, I. and Richaud, C. (1993). Physical mapping of the scattered methionine genes on the Escherichia coli chromosome. *J Bacteriol* 175, 3689-3691.
  12. Saint Girons, I., Duchange, N., Cohen, G.N. and Zakin, M.M. (1984). Structure and autoregulation of the metJ regulatory gene in Escherichia coli. *J Biol Chem* 259, 14282-14285.
  13. Phillips, S.E.V., Manfield, I., Parsons, I., Davidson, B.E., Rafferty, J.B., Somers, W.S., Margarita, D., Cohen, G.N., Saint Girons, I. and Stockley, P.G. (1989). Co operative tandem binding of met repressor of Escherichia coli. *Nature* 341, 711-715.
  14. Phillips, S.E.V., and Stockley, P.G. (1996). Structure and function of Escherichia coli met repressor: similarities and contrasts with trp repressor. *Phil Trans R Soc Lond B* 351, 527-535.
  15. He, Y.Y., Stockley P.G. and Gold, L. (1996). In vitro evolution of the DNA binding sites of Escherichia coli methionine repressor, MetJ. *J Mol Biol* 255, 55-66.
  16. Rafferty, J.B., Somers, W.S., Saint Girons, I. and Phillips, S.E.V. (1989). Three dimensional crystal structures of the Escherichia coli Met repressor with and without co repressor. *Nature* 341, 705-710.
  17. Phillips, K., and Phillips, S.E.V. (1994). Electrostatic activation of E. coli methionine repressor. *Structure* 2, 309-316.
  18. Parsons, I.D., Persson, B., Mekhelfia, A., Blackburn, G.M., and Stockley, P.G. (1995). Probing the molecular mechanism of action of co-repressor in the E. coli methionine repressor operator complex using surface plasmon resonance. *Nucleic Acids Res*, 211-216.
  19. Phillips, S.E.V., and Stockley, P.G. (1994). Similarity of met and trp repressors. *Nature* 368, 160.

20. Otwinowski, Z., Schevitz, R.W., Zhang, R.G., Lawson, C.L., Joachimiak, A., Marmorstein, R.Q., Luisi, B.F. and Sigler, P.B. (1988). Crystal structure of trp repressor/operator complex at atomic resolution. *Nature* 335.
21. Zheng, M., Wang, X., Templeton, L.J., Smulski, D.R., LARossa, R.A. and Storz, G. (2001). DNA microarray mediated transcriptional profiling of the *Escherichia coli* response to hydrogen peroxide. *J Bacteriol* 183, 4562-4570.
22. Wei, Y., Lee, J M., Richmond, C., Blattner, F.R., Rafalski, J.A. and LARossa, R.A (2001). High-Density Microarray-Mediated Gene Expression Profiling of *Escherichia coli*. *J Bacteriol* 183, 545-556.
23. Richmond, C.S., Glasner, J.D., Mau, R., Jin, H. and Blattner, F.R. (1999). Genome wide expression profiling in *Escherichia coli* K 12. *Nucleic Acids Res* 27.
24. Zimmer, D.P., Soupene, E., Lee, H.L., Wendish, V.F., Khodursky, A.B., Peter, B.J., Bender, R.O. and Kustu, S. (2000). Nitrogen regulatory protein C controlled genes of *Escherichia coli*: scavenging as a defense against nitrogen limitation. *Proc Natl Acad Sci (USA)* 97, 14674-14679.
25. Oh, M.K., Rohlin, L., Kao, K.C. and Liao, J.C. (2002). Global expression profiling of acetate grown *Escherichia coli*. *J Biol Chem* 277, 13175-13183.
26. Schembri, M.A., Ussery, D.W., Workman, C., Hasman, H. and Klemm, P. (2002). DNA microarray analysis of fim mutations in *Escherichia coli*. *Mol Genet Genomics* 267, 721-729.
27. DELisa, M.P., Wu, C F., Wang, L., Valdes, J.J. and Bentley, W.E. (2001). DNA microarray based identification of genes controlled by autoinducer 2 stimulated quorum sensing in *Escherichia coli*. *J Bacteriol* 183, 5239-5247.
28. Khodursky, A.B., Peter, B.J., Cozzarelli, N.R., Botstein, D., Brown, P.O. and Yanofsky, C. (2000). DNA microarray analysis of gene expression in response to physiological and genetic changes that affect tryptophan metabolism in *Escherichia coli*. *Proc Natl Acad Sci(USA)* 97, 12170-12175.
29. Hung, S.P., Baldi, P. and Hatfield G.W. (2002). The effects of leucine responsice regulatory protein. *J Biol Chem* 277, 40309-40323.
30. He, Y.Y., Garvie, C.W., Elworthy, S., Manfield, I.W., McNally, T., Lawrenson, I.D., Phillips, S.E.V. and Stockley, P.G. (2002). Structural and functional studies of an intermediate on the pathway to operator binding by *Escherichia coli* MetJ. *J Mol Biol* 320, 39-53.

31. Marincs, F., McDowall, K.J. & Stockley, P.G. (2004). A combined in vitro transposition-in vivo recombination mutagenesis method to knock out genes in *Escherichia coli*. *Am Biotech Lab* 22, 8-10.
32. Yu, D., Ellis, H.M., Lee, E C., Jenkins, N.A., Copeland, N.G. and Court, D.L. (2000). An efficient recombination system for chromosome engineering in *Escherichia coli*. *Proc Nat Acad Sci (USA)* 97, 5978-5983.
33. Dudoit, Y., Yang, Y.H., Callow, M.J. and Speed, T.P. (2000). Statistical methods for identifying differentially expressed genes in replicated cDNA microarray experiments. Technical Report 578, Department of Statistics, UC Berkeley, CA.
34. Cleveland, W.S. (1981). *The American Statistician*, 35, 54.
35. Pasanen, T., Saarela, J., Saarikko, I., Toivanen, T., Tolvanen, M., Vihinen, M. and Wong, G. (2003). DNA Microarray Data Analysis: CSC - Scientific Computing Ltd. ( available on line : <http://www.csc.fi/oppaat/siru/>), 100-102.
36. Merlin, C., Gardiner, G., Durand, S. and Masters, M. (2002). The *Escherichia coli* metD locus encodes an ABC transporter which includes Abc (MetN), YaeE (MetI), and YaeC (MetQ). *J Bacteriol* 184, 5513-5517.
37. Gál, J., Szvetnik, A., Schnell, R. and Kálmán, M. (2002). The metD D methionine transporter locus of *Escherichia coli* is an ABC transporter gene cluster. *J Bacteriol* 184, 4930-4932.
38. Salgado, H., Gama-Castro, S., Martinez-Antonio, A., Diaz-Peredo, E., Sanchez-Solano, F., Peralta-Gil, M., Garcia-Alonso, D., Jimenez-Jacinto, V., Santos-Zavaleta, A., Bonavides-Martinez, C., Collado-Vides, J. (2004). RegulonDB (version 4.0): transcriptional regulation, operon organization and growth conditions in *Escherichia coli* K-12. *Nucleic Acids Res.* 32, D303-D306.
39. Tanabe, H., Goldstein, J., Yang, M., Inouye, M.J. (1992). Identification of the promoter region of the *Escherichia coli* major cold shock gene, cspA. *J. Bacteriol.* 174, 3867-3873.
40. Liu, R., Blackwell, T.W. and States, D.J. (2001). Conformational model for binding site recognition by the *E. coli* MetJ transcription factor. *Bioinformatics* 17, 622-633.
41. Wendisch, V.F., Zimmer, D.P., Khodursky, A., Peter. B., Cozzarelli, N., and Kustu, S. (2001). Isolation of *Escherichia coli* mRNA and comparison of

- expression using mRNA and total RNA on DNA microarrays. *Anal Biochem.* 290, 205-213.
42. Parsons, I.D., and Stockley, P.G. (1997). Quantitation of the *Escherichia coli* methionine repressor-operator interaction by surface plasmon resonance is not affected by the presence of a dextran matrix. *Anal Biochem.* 254, 82-87.
  43. Cai XY, M.M., Redfield B, Glass R, Brot N, and Weissbach H (1989). Methionine synthesis in *Escherichia coli*: effect of the MetR protein on metE and metH expression. *Proc Natl Acad Sci (USA)* 86, 4407-4411.
  44. Stockley, P.G., Baron, A.J., Wild, C.M., Parsons, I.D., Miller, C.M., Holtham, C.A.M., and Baumberg, S. (1998). Dissecting the molecular details of prokaryotic transcriptional control by surface plasmon resonance: the methionine and arginine repressor proteins. *Biosensors Bioelect* 13, 637-650.
  45. Kuo, W.P., Jenssen, T.K., Butte, A.J., Ohno Machado, L. and Kohane, I.S. (2002). Analysis of matched mRNA measurements from two different microarray technologies. *Bioinformatics* 18, 405-412.
  46. Lawson, C.L., and Carey, J. (1993). Tandem binding in crystals of a trp repressor/operator half-site complex. *Nature* 366, 178-182.
  47. Gold, L., Brown, D., He, Y., Shtatland, T., Singer, B.S. and Wu, Y. (1997). From oligonucleotide shapes to genomic SELEX: Novel biological regulatory loops. *Proc Natl Acad Sci (USA)* 94, 59-64.
  48. Lawrenson, I.D., and Stockley, P.G. (2004). Kinetic analysis of operator binding by the *E. coli* methionine repressor highlights the role(s) of electrostatic interactions. *FEBS Letters* 564, 136-142.
  49. Greene, R.C. (1996). Biosynthesis of Methionine. In *Escherichia coli* and *Salmonella typhimurium*: Cellular and Molecular Biology. F.C. Neidhardt (editor-in-chief). 2nd ed. Washington D.C.: ASM Press,, 542-560.

#### WEBSITE REFERENCES:

Introduction to EZ::TN™ Transposon Tools for Transposomics™. URL

[http://www.epicentre.com/guide\\_to\\_transposomics.asp](http://www.epicentre.com/guide_to_transposomics.asp)

MWG *E. coli* K12 array V2 spotting pattern. URL

[http://ecom2.mwgdna.com/download/arrays/arrays/gene\\_id/html/gene\\_id\\_ecoli\\_v2.html](http://ecom2.mwgdna.com/download/arrays/arrays/gene_id/html/gene_id_ecoli_v2.html)



## TABLE LEGENDS

Table 1. The genome-wide effects of knocking out *metJ*. Strains LU106(pFM26) and LU106(pFM20) were compared using an oligonucleotide-based array of 4,288 *E. coli* genes. Ratios are for three independent experiments. Only those genes with an average expression ratio  $\geq 1.8$  are shown. Genes within the known methionine regulon are shown in boldface, the array designations of *metN* and *metI* are also shown in brackets. The de-repression ratios for all genes on this array are shown in Table 7 of Supplementary Material.

Table 2. Expression ratios of genes relevant to methionine biosynthesis on the PCR-based microarray. Data are average values from three independent samples for experiments comparing strain LU106 (*metJ*<sup>-</sup>) versus DY378 (wt), and strain LU106/pFM26 (*metJ*<sup>-</sup>) versus strain LU106/pFM20 (*metJ*<sup>+</sup>).

<sup>a</sup> Ratios are for three independent experiments that each averaged the values calculated from six parallel spots on a single slide. Ratios for other genes are shown in Table 6 of Supplementary Material.

Table 3. Gene expression ratios in *metJ* mutant Q44K strain versus wild-type. Data for the *met* regulon comparing wild-type (LU106/pFM20 (*metJ*<sup>+</sup>)) vs. Q44K (LU106/pFM45 (*metJQ44K*<sup>+</sup>)) strains. Experimental details as in Table 2 and Materials and Methods.

## FIGURE LEGENDS

Figure 1. Components of the *E. coli* methionine biosynthesis pathway.

A) Structure of the repressor-operator complex. Cartoon representation of a single repressor dimer bound to a single met-box operator (framework model) within the higher order complex (PDB 1cma) [2]. The positions of the mutated protein side-chains analysed here are shown as stick models (one labelled) on a ribbon backbone of a single repressor dimer (chains in light and dark grey). AdoMet omitted for clarity.  
B) Architecture of well known *met* promoters of *E. coli* [49]. The positions of the

promoters for the genes labelled are indicated by open boxes. Arrowheads show the positions of the start codons and the direction of transcription. Note, the multiple promoters for *metA* & *metJ*, some of which do not overlap operators. Note also the multiple operator sites for *metE*. C) The biosynthetic pathway for methionine showing the gene product operating at each step [11].

Figure 2. EMSA Assays for Non-*met* Gene Operators.

Samples were: Lanes 1 to 4: *metC*, [MetJ dimer] = 0, 1, 2 & 4 nM, respectively; Lanes 5 to 9: *folE*, = 0, 30, 40, 50 & 80 nM, respectively; Lanes 10 to 14: *cspA*, = 0, 30, 40, 50 & 80 nM, respectively; Lanes 15 to 19: *yaeS* (from a separate gel), = 0, 15, 30, 80 & 200 nM, respectively.

The sequences of the oligonucleotide substrates used were as follows, the underlined bases being identities to the met-box consensus, vertical lines indicate junctions between putative met-boxes:

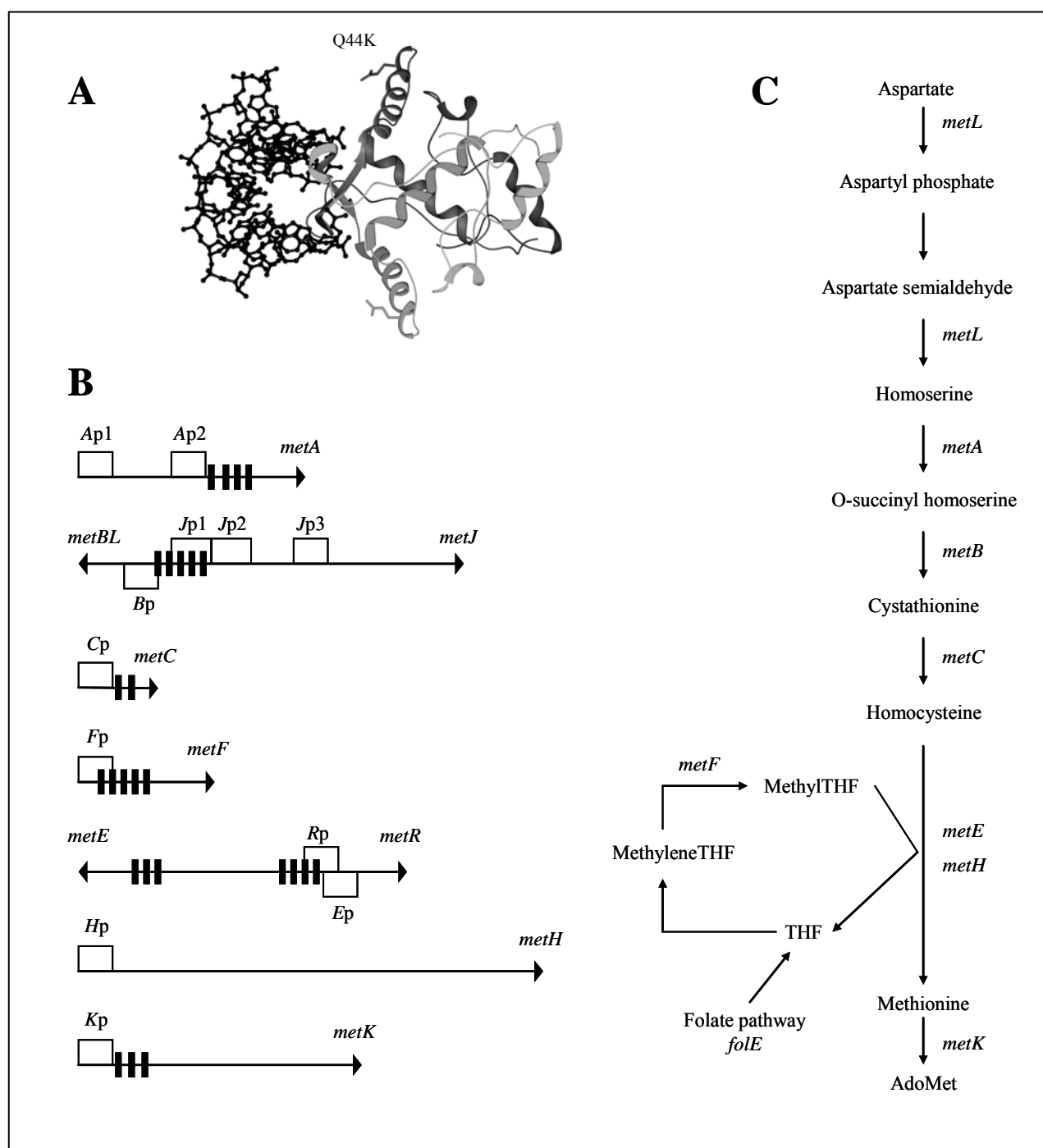
*metC*, 5'-CATGCTAGTTT|AGACATCC|AGACGTAT|AAAAACAGGAA;  
*folE*, 5'-TATTTGCATAA|CGATGTTT|TAACATCT|GCTGATGAAAG;  
*yaeS*, 5'-CCACAATGTGT|GGACGATG|TGTTATCT|GTTGATGC|GAACGCGCGTG;  
*cspA*, 5'-TAATGCACAT|CAACGGTT|TGACGTAC|AGACCATT|AAAGCAGTGTA

Figure 3. RT-PCR analysis of *met* transcripts.

M indicates marker lanes containing a 100 bp ladder; c: lanes where aliquots have been loaded of control assays in which reverse transcriptase was omitted; R: a sample from LU106 (pFM20) cells in which the *met* genes are repressed; D: a sample from LU106 (pFM26) cells in which there is no functional *metJ* gene and consequently expression of *met* genes is derepressed. The transcripts being assayed are indicated at the top of each panel.



### Figure 1



**Figure 2**

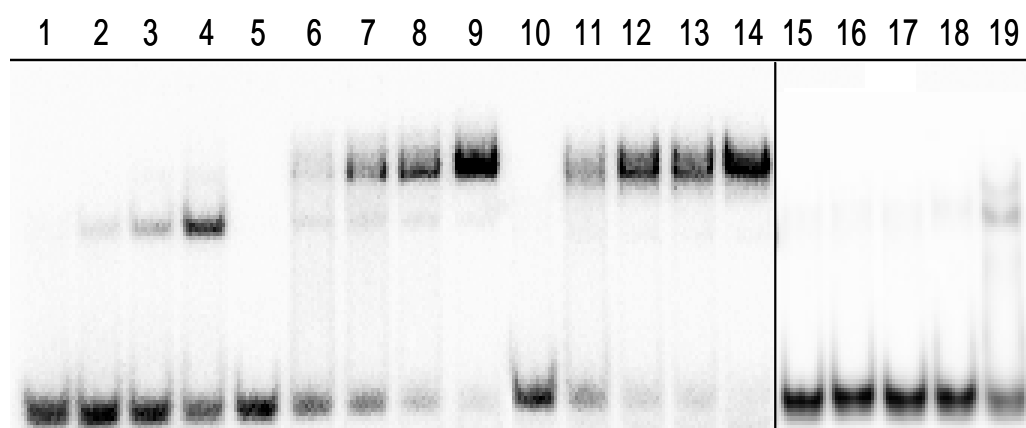
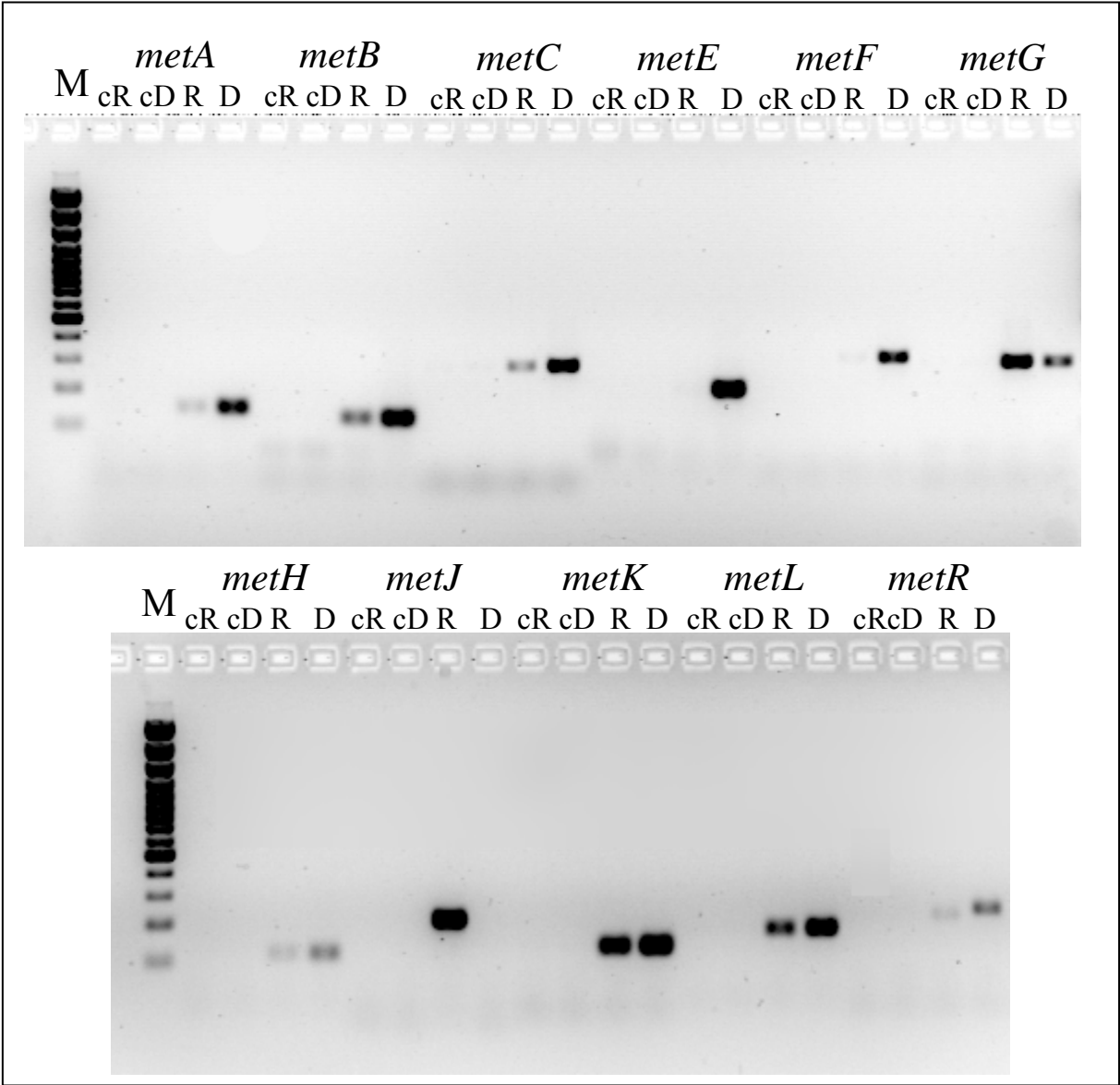


Figure 3



**Table 1**

Derepression Ratio  
LU106-pFM26/LU106-pFM20

Gene	(Ave±SD)
<b><i>metE</i></b>	<b>34.1±14.5</b>
<i>yaeS</i>	5.3 ±0.9
<b><i>metI(yaeE)</i></b>	5.1 ±1.4
<i>lit</i>	4.9 ±3.3
<b><i>metB</i></b>	<b>4.5 ±0.1</b>
<i>folE</i>	3.9 ±0.7
<i>cspA</i>	3.8 ±1.9
<b><i>metF</i></b>	<b>3.5 ±0.6</b>
<b><i>metK</i></b>	<b>3.5 ±0.9</b>
<i>b0539</i>	3.1 ±1.6
<i>polB</i>	2.8 ±1.2
<i>prpD</i>	2.8 ±0.6
<i>yi82</i>	2.8 ±0.5
<b><i>metN(abc)</i></b>	2.6 ±0.8
<i>b1240</i>	2.6 ±1.3
<i>ydcN</i>	2.3 ±0.8
<b><i>metA</i></b>	<b>2.0 ±0.6</b>
<i>yeaO</i>	1.8 ±0.3
<b><i>metR</i></b>	<b>1.8 ±0.4</b>
<i>narV</i>	1.8±0.1

**Table 2**

Gene	LU106/DY378 Ave±SD <sup>a</sup>	LU106-pFM26/LU106-pFM20 Ave±SD <sup>a</sup>
metA	7.2±1.0	3.8±0.3
metB	3.5±0.2	2.8±0.4
metC	2.7±0.2	2.6±0.5
metE	1.3±0.1	37.7±2.8
metF	5.2±0.3	7.8±1.0
metG	1.1±0.1	0.9±0.2
metH	1.0±0.2	1.3±0.2
metJ	2.6±0.3	0.5±0.1
metK	8.2±1.0	4.6±0.6
metL	1.5±0.2	2.5±0.5
metR	1.8±0.2	1.4±0.2

**Table 3**

Gene LU106-pFM45 / LU106-pFM20  
Ave±SD

---

<i>metA</i>	1.6±0.1
<i>metB</i>	1.5±0.2
<i>metC</i>	1.3±0.04
<i>metE</i>	5.7±0.3
<i>metF</i>	1.5±0.1
<i>metG</i>	1.2±0.2
<i>metH</i>	1.6±0.1
<i>metJ</i>	7.0±0.1
<i>metK</i>	1.6±0.1
<i>metL</i>	1.3±0.1
<i>metR</i>	1.3±0.1

---